Journal of
Applied Remote Sensing

RemoteSensing.SPIEDigitalLibrary.org

Advances in multiangle satellite remote sensing of speciated airborne particulate matter and association with adverse health effects: from MISR to MAIA

David J. Diner
Stacey W. Boland
Michael Brauer
Carol Bruegge
Kevin A. Burke
Russell Chipman
Larry Di Girolamo
Michael J. Garay
Sina Hasheminassab
Edward Hyer
Michael Jerrett
Veljko Jovanovic
Olga V. Kalashnikova
Yang Liu
Alexei I. Lyapustin
Randall V. Martin
Abigail Nastan
Bart D. Ostro
Beate Ritz
Joel Schwartz
Jun Wang
Feng Xu

David J. Diner, Stacey W. Boland, Michael Brauer, Carol Bruegge, Kevin A. Burke, Russell Chipman, Larry Di Girolamo, Michael J. Garay, Sina Hasheminassab, Edward Hyer, Michael Jerrett, Veljko Jovanovic, Olga V. Kalashnikova, Yang Liu, Alexei I. Lyapustin, Randall V. Martin, Abigail Nastan, Bart D. Ostro, Beate Ritz, Joel Schwartz, Jun Wang, Feng Xu, "Advances in multiangle satellite remote sensing of speciated airborne particulate matter and association with adverse health effects: from MISR to MAIA," *J. Appl. Remote Sens.* **12**(4), 042603 (2018), doi: 10.1117/1.JRS.12.042603.

SPIE.

Advances in multiangle satellite remote sensing of speciated airborne particulate matter and association with adverse health effects: from MISR to MAIA

David J. Diner,[a,*] Stacey W. Boland,[a] Michael Brauer,[b] Carol Bruegge,[a] Kevin A. Burke,[a] Russell Chipman,[c] Larry Di Girolamo,[d] Michael J. Garay,[a] Sina Hasheminassab,[e] Edward Hyer,[f] Michael Jerrett,[g] Veljko Jovanovic,[a] Olga V. Kalashnikova,[a] Yang Liu,[h] Alexei I. Lyapustin,[i] Randall V. Martin,[j,k] Abigail Nastan,[a] Bart D. Ostro,[l] Beate Ritz,[g] Joel Schwartz,[m] Jun Wang,[n] and Feng Xu[a]

[a]Jet Propulsion Laboratory, California Institute of Technology, Pasadena, California, United States
[b]University of British Columbia, School of Population and Public Health, Vancouver, British Columbia, Canada
[c]University of Arizona, College of Optical Sciences, Tucson, Arizona, United States
[d]University of Illinois Urbana-Champaign, Department of Atmospheric Science, Urbana, Illinois, United States
[e]South Coast Air Quality Management District, Diamond Bar, California, United States
[f]Naval Research Laboratory, Marine Meteorology Division, Monterey, California, United States
[g]University of California Los Angeles, Fielding School of Public Health, Los Angeles, California, United States
[h]Emory University, Rollins School of Public Health, Atlanta, Georgia, United States
[i]NASA Goddard Space Flight Center, Climate and Radiation Laboratory, Greenbelt, Maryland, United States
[j]Dalhousie University, Department of Physics and Atmospheric Science, Halifax, Nova Scotia, Canada
[k]Smithsonian Astrophysical Observatory, Cambridge, Massachusetts, United States
[l]University of California Davis, Air Quality Research Center, Davis, California, United States
[m]Harvard University, Department of Epidemiology, Boston, Massachusetts, United States
[n]University of Iowa, College of Engineering, Iowa City, Iowa, United States

Abstract. Inhalation of airborne particulate matter (PM) is associated with a variety of adverse health outcomes. However, the relative toxicity of specific PM types—mixtures of particles of varying sizes, shapes, and chemical compositions—is not well understood. A major impediment has been the sparse distribution of surface sensors, especially those measuring speciated PM. Aerosol remote sensing from Earth orbit offers the opportunity to improve our understanding of the health risks associated with different particle types and sources. The Multi-angle Imaging SpectroRadiometer (MISR) instrument aboard NASA's Terra satellite has demonstrated the value of near-simultaneous observations of backscattered sunlight from multiple view angles for remote sensing of aerosol abundances and particle properties over land. The Multi-Angle Imager for Aerosols (MAIA) instrument, currently in development, improves on MISR's sensitivity to airborne particle composition by incorporating polarimetry and expanded spectral range. Spatiotemporal regression relationships generated using collocated surface monitor and chemical transport model data will be used to convert fractional aerosol optical depths retrieved from MAIA observations to near-surface PM_{10}, $PM_{2.5}$, and speciated $PM_{2.5}$. Health scientists on the MAIA team will use the resulting exposure estimates over globally distributed target areas to investigate the association of particle species with population

*Address all correspondence to: David J. Diner, E-mail: David.J.Diner@jpl.nasa.gov

 [DOI: 10.1117/1.JRS.12.042603]

Keywords: particulate matter; aerosols; remote sensing; human health.

Paper 180287SS received Apr. 7, 2018; accepted for publication Jun. 26, 2018; published online Jul. 28, 2018.

1 Introduction

Numerous epidemiological investigations have provided compelling evidence that inhalation of airborne particulate matter (PM) reduces life expectancy and contributes to myriad other health problems including heart disease, stroke, respiratory impairment, lung cancer, diabetes, cognitive decline, and adverse birth outcomes.[1–5] The Global Burden of Disease (GBD) study[6–8] ranks ambient $PM_{2.5}$ (particles <2.5 μm in aerodynamic diameter) as the top environmental risk factor worldwide, causing about 4.1 million premature deaths in 2016. Although GBD and many other studies have focused on human exposure to the total mass of $PM_{2.5}$, the relative toxicity of specific PM types—particle mixtures with different size distributions and chemical compositions—remains less well understood.[9,10] As these types often have different sources, this is a major impediment to targeting interventions that would improve public health.

Airborne PM is a complex mixture of particles with different sizes, shapes, and chemical compositions, originating from multiple sources and subject to dynamic atmospheric transformations. The challenges associated with studying the health impacts of different PM types are due, in part, to the heterogeneity of particle properties and their variability in space and time. Although surface monitors provide the most accurate means available for measuring PM mass concentrations and chemical compositions at fixed locations, they are unavailable in many parts of the developing world. Monitors capable of measuring PM speciation are especially uncommon and, even when available, lack the spatial density needed to assess fine-scale exposure gradients. As noted by the World Bank,[11] "Scarce public resources have limited the monitoring of atmospheric PM concentrations in developing countries, despite their large potential health effects. As a result, policymakers ... remain uncertain about the exposure of their residents to PM air pollution."

The US National Academy of Sciences has placed a priority on improving our understanding of the relative toxicity of different types of PM.[12] Surface monitors alone, particularly those capable of measuring speciated PM, are not sufficient to achieve this objective as they are too sparsely distributed and expensive to install and maintain. Inaccurate exposure estimates can result when PM concentrations vary over spatial scales smaller than the distances between monitors.[13] Although PM exposure over a scale of a few hundred meters can be important for individuals who live near pollution sources (such as major roadways) or who have limited mobility (e.g., residents of nursing homes), recent geostatistical studies suggest that most PM spatial variability is adequately sampled at scales ranging from 1 to 4 km.[14,15] The US Environmental Protection Agency (EPA) notes that "the use of central fixed-site monitors to represent population exposure" is a key factor limiting our knowledge as to which PM types pose the greatest health risks,[10] and recommends monitoring of urban PM at the neighborhood scale (0.5 to 4.0 km) as it represents conditions where people commonly live and work.[16]

Satellite remote sensing—in combination with surface monitor measurements and chemical transport model (CTM) outputs—currently offers a practical approach to frequent, neighborhood-scale mapping of $PM_{2.5}$ mass concentrations around the world. The US EPA and National Institute of Environmental Health Sciences highlight the value of remote sensing to "augment ground-based air quality sampling and help fill pervasive data gaps that impede efforts to study air pollution and protect public health."[17] $PM_{2.5}$ mass estimates derived from satellite observations are proving useful in epidemiological studies.[18,19] Because PM speciation monitors are even less common (and more expensive) than those measuring total mass concentrations, future advances in satellite capability to characterize particle type, and extension of current methodologies to handle speciation, have the potential to improve our understanding of which PM

mixtures and sources are most harmful. This information could help prioritize air quality guidelines, facilitate cost-effective monitoring and mitigation strategies, and aid research into the biological mechanisms for documented PM health effects.[12]

The Weather and Air Quality panel of the 2017 Decadal Survey for Earth Science and Applications from Space[20] includes among its highest priority objectives improvement in the ability to estimate global air pollution impacts on human health along with the "establishment and maintenance of a robust, comprehensive observing strategy for the spatial distribution of PM (including speciation)." Given that the particles responsible for human health risks are situated near ground level, the Decadal Survey recognizes the need for an integrated strategy that combines space-based, aircraft, and ground-based observations, augmented by data from CTMs.

The past two decades have witnessed major advances in our ability to map aerosol abundances and particle properties from space. Aerosol retrievals over land from instruments, such as the Multi-angle Imaging SpectroRadiometer (MISR),[21] Moderate resolution Imaging Spectroradiometer (MODIS),[22] and Sea-viewing Wide Field-of-view Sensor (SeaWiFS)[23] have been successfully used to generate global maps of near-surface fine PM concentrations and track multiyear trends.[24,25] These satellite-based maps of fine PM have been used in the GBD and many other health impact studies, including several that examined $PM_{2.5}$ exposure and lung function, kidney disease, lung cancer, breast cancer, heart attacks, and birth outcomes.[7,8,26–32] These efforts have been made possible by advances in spaceborne instrumentation and associated data processing algorithms.

Current efforts in aerosol remote sensing are aimed at improving our ability to characterize particle type. Multiangle observing, implemented in satellite instruments such as MISR[33] and Polarization and Directionality of Earth's Reflectances (POLDER),[34] has been shown to provide an effective modality for achieving this objective.[21,35,36] The MISR instrument, built by the Jet Propulsion Laboratory (JPL) for flight on NASA's Terra spacecraft, has been collecting Earth science data since February 2000. In this paper, we briefly review the application of MISR to aerosol and PM remote sensing. This discussion serves as a prelude to a description of the Multi-Angle Imager for Aerosols (MAIA),[37] which builds upon MISR heritage and is currently in development at JPL. Key elements of the MAIA investigation include (1) a satellite instrument that incorporates a number of measurement advances relative to MISR, such as expanded spectral range and polarimetric imaging, (2) integration of space-based and ground-based measurements and CTM outputs to generate high-resolution maps on a 1-km spatial grid of speciated PM in a selected set of globally distributed target areas, and (3) linkage of the resulting PM exposure data to human health records to assess the impact on disease. This paper is intended to familiarize the scientific and public health communities and potential data users with the principal elements and strategies to be employed by the MAIA investigation, and to provide an overview of the current development status of the project.

2 Multi-angle Imaging SpectroRadiometer

2.1 *Background*

The MISR instrument[33] was launched into polar, sun-synchronous orbit aboard NASA's Terra spacecraft on December 18, 1999. Routine Earth observations began on February 24, 2000. MISR uses nine separate cameras to image the Earth at nine discrete view angles: 0 deg (nadir) and 26.1 deg, 45.6 deg, 60.0 deg, and 70.5 deg forward and backward of nadir. Pushbroom imagery at 275-m- to 1.1-km spatial resolution over a 400-km-wide swath is acquired in four visible/near-infrared (VNIR) spectral bands (446, 558, 672, and 866 nm) in each camera by making use of spacecraft motion and linear detector arrays. MISR was designed to improve our understanding of the Earth's climate, ecology, and environment. The suite of validated geophysical data products[38] is generated and archived for public distribution at the NASA Langley Atmospheric Science Data Center (ASDC). An extensive bibliography of peer-reviewed publications describing, applying, and validating MISR data for studies of aerosol climate, air quality, and health impacts, radiation and cloud–climate interactions, cloud-tracked winds, and surface biospheric and cryospheric science is available on the MISR website.[39]

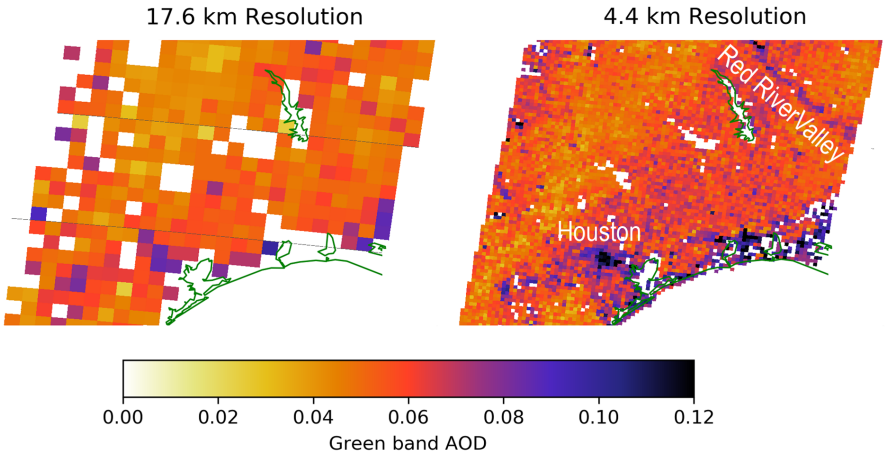

Fig. 1 Example comparison of 17.6-km (V22) and 4.4-km (V23) MISR AOD retrieval.

2.2 *Aerosol Data Product Generation*

Among the objectives of the MISR investigation is global mapping of aerosols. Direct radiative effects of aerosols, both in magnitude and sign, depend principally on the aerosol optical depth (AOD), single scattering albedo, scattering phase function, and the albedo of the underlying surface. Aerosols also have indirect climate and hydrological impacts through their effects on the albedos, lifetimes, and microphysical properties of clouds, and play a major role in human and environmental health.

Multiangle radiance observations are valuable for enhancing the aerosol signal relative to surface reflection and providing sensitivity to the aerosol scattering phase functions, which are governed by particle size, shape, and composition.[40–42] Radiative-transfer-based algorithms are applied to radiometrically calibrated, georectified, and cloud-screened MISR multiangle, multispectral imagery to generate the aerosol product. Over land, two main algorithms work together. The first, known as heterogeneous land, utilizes spatial contrasts to derive an empirical orthogonal function representation of the surface contribution to the measured multiangle radiances.[43] The second, known as homogeneous land, uses similarity in the angular shape of surface bidirectional reflectance factors (BRFs) among the four spectral bands as a constraint on the aerosol retrievals.[44] Both algorithms make use of the multiangular nature of the MISR observations. By employing a lookup table consisting of 74 mixtures of aerosol particles having prescribed microphysical and optical properties and using several goodness-of-fit metrics to compare modeled top-of-atmosphere radiances to the MISR observations, the retrieval algorithm provides sensitivity to both AOD and aerosol types.[35]

2.3 *Application to Air Quality and Human Health*

Comparisons of MISR AODs with independent ground-based sunphotometer AODs from the Aerosol Robotic Network (AERONET)[45] show a high positive correlation,[46,47] including over arid land and urban areas.[48–50] As a result, MISR is one of several satellite instruments contributing to widely used global maps of $PM_{2.5}$.[24,25,51] MISR's sensitivity to particle type enables separation of anthropogenic aerosols from dust, which has led to improved estimates of ground-level $PM_{2.5}$ concentrations in the arid western United States compared with single-angle approaches.[52,53] These multivariate regression models were initially developed to explore MISR's ability to quantitatively characterize ground-level concentrations of $PM_{2.5}$ components such as sulfate, nitrate, organic carbon (OC), and elemental carbon (EC). Later, a more flexible generalized additive model (GAM) using MISR fractional AOD (partitioned by particle properties) scaled by vertical profiles of aerosol loading from the GEOS-Chem transport model was able to explain 70% of the variability in sulfate concentrations measured by surface monitors.[54] Particle size and shape information from MISR retrievals has been used to associate anthropogenic pollution with significant decadal rise in AOD and ground-level $PM_{2.5}$ over urban centers and densely populated rural areas in India.[55,56]

Validation of MISR aerosol retrievals using the operational 17.6-km resolution product demonstrated high accuracy over land for AOD <0.5 and systematic underestimation (though high correlation) at high aerosol loading.[46–50] Hierarchical Bayesian modeling and statistical analysis of this product suggested potential benefits of going to higher spatial resolution.[57,58] Given the value of finer spatial detail for studies of urban air quality, the MISR retrieval algorithm was recently adapted to operate on a 4.4-km spatial grid, and prototyping of the updated code demonstrated significant improvements in terms of accuracy, coverage, and mapping of spatial gradients.[59] Consequently, the operational aerosol product was upgraded from 17.6-km (version 22) to 4.4-km spatial resolution (version 23), and the V23 product was made publicly available in late 2017. An example of the improvement in spatial resolution and coverage is shown in Fig. 1. These data are from a Terra overpass of southeastern Texas and western Louisiana on February 14, 2013. The 4.4-km resolution product does a superior job in pinpointing elevated AODs over Houston and the Red River Valley.

Prototype versions of MISR's 4.4-km aerosol product have been used over parts of southern and central California to estimate daily-averaged $PM_{2.5}$, PM_{10}, and speciated $PM_{2.5}$ concentrations. Through leave-one-out cross-validation against the EPA's federal reference method measurements, the product was shown to capture $PM_{2.5}$ spatial variability at the grid scale and to separate $PM_{2.5}$ and PM_{10} size modes in the greater Los Angeles area.[60] Another recent study applied GAMs to 15 years of the prototype 4.4-km product, and showed that the GAMs are able to explain 66%, 62%, 55%, and 58% of the variability in daily-averaged $PM_{2.5}$ sulfate, nitrate, OC, and EC concentrations.[61]

3 Multi-Angle Imager for Aerosols

3.1 *Background*

NASA selected the MAIA investigation in 2016 as part of its Earth Venture Instrument program. The MAIA instrument builds upon MISR's legacy and adds new measurement capabilities for determining concentrations of total fine ($PM_{2.5}$) and coarse ($PM_{10} - PM_{2.5}$) particles, along with the amounts of hydrated nonorganics, OC, black carbon (BC) or EC, and mineral dust in the fine particle mixtures. An integrated satellite/surface-level data and modeling strategy[62] is used to generate daily mean PM values on a 1-km grid. This approach enables further separating the nonorganics into sulfate and nitrate contributions. The main challenges that MAIA aims to address are to demonstrate that current satellite-based strategies for mapping total $PM_{2.5}$ mass can be extended to include speciation, and that the approach can be implemented on an operational basis.

MAIA's primary objective is to assess the impacts of different types of airborne PM on human health. The planned investigation consists of several elements: (1) the MAIA satellite instrument, (2) algorithms and software to generate PM maps using data from the MAIA instrument, surface monitors, and CTMs, and (3) epidemiological studies using the MAIA PM maps and geocoded health data to associate different types of PMs with adverse health outcomes. By increasing the density of spatial sampling and the coverage of PM in the targeted regions, MAIA overcomes a major impediment faced by prior studies that have examined the health impacts of specific PM types,[63–67] namely their limited ability to accurately assess exposure due to the small number of ground-based speciated PM monitors. To support other atmospheric science research, MAIA plans to collect measurements over areas that are of value for studying aerosol and cloud impacts on Earth's climate, and over extreme events such as wildfires, dust storms, and erupting volcanoes. Demonstration in Earth orbit of the new imaging technologies used in the MAIA instrument will also benefit NASA's planning for future missions.

3.2 *Instrument Design*

The MAIA instrument is designed to combine multispectral, polarimetric, and multiangular capabilities into a single, integrated imaging system capable of mapping total and speciated PM at the neighborhood scale. At the heart of the instrument is a pushbroom camera mounted on a two-axis gimbal.

3.2.1 *Spectral coverage*

MAIA's camera includes spectral bands in the ultraviolet (UV), VNIR, and shortwave infrared (SWIR), which improves sensitivity to aerosol particle properties compared with MISR's VNIR-only bands. UV wavelengths are useful for detecting absorption by hematite and aluminum oxide in dust particles, nitrated aromatic and polycyclic aromatic hydrocarbons in organic aerosols (e.g., brown carbon), and BC or EC (soot).[68,69] The use of VNIR bands for fine aerosols draws upon MISR, MODIS, and POLDER heritage. The SWIR is sensitive to coarse aerosols,[70] and a band located in a strong water vapor absorption feature provides enhanced cirrus screening.[71] Channels within and near the O_2 A-band are included to explore sensitivity to aerosol layer (and cloud) height.[72,73] Table 1 summarizes the MAIA spectral band set.

3.2.2 *Polarimetry*

As shown in Table 1, three of the MAIA bands are polarimetric, providing additional sensitivity to particle size and compositional proxies, such as refractive index.[74–76] By constraining these particle properties, polarization also works in conjunction with radiance to constrain aerosol absorption.[77] To capitalize on the benefits of polarimetry in future instruments, the aerosol community has established an uncertainty requirement of ± 0.005 in degree of linear polarization,[78] which is more than three times stricter than POLDER performance. The MAIA camera achieves this level of accuracy at a spatial resolution of 1 km (compared to 6 km with POLDER) by using a polarization modulation technique enabled by a pair of photoelastic modulators and a pair of achromatic quarter-wave plates.[79,80] This results in a time-varying oscillation in the plane of linear polarization at a frequency near 27.5 Hz. The readout integrated circuit enables rapid sampling of the modulated signals during each pushbroom image frame. Silicon detectors are used in the UV/VNIR and mercury–cadmium–telluride detectors in the SWIR. Above the detector array is a set of spectral filters and wiregrid polarization analyzers. A similar system operating in the UV/VNIR has been implemented in JPL's Airborne Multiangle SpectroPolarimetric Imager (AirMSPI).[81] The second-generation AirMSPI-2 extends the spectral range into the SWIR.[82] MAIA makes use of heritage from both airborne instruments.

Table 1 MAIA spectral bands.

Band center (nm)	Bandwidth (nm)	Polarimetric	Purpose (s)	Legend for spectral band purposes
365	37		1	1. Aerosol spectral absorption and height
391	39		1	2. Aerosol fine mode size distribution
415	39		1	3. Aerosol refractive index
444	53	*x*	1, 2, 3, 8	4. Water vapor absorption
550	43		2, 8, 9	5. Bracket absorption bands
646	72	*x*	1, 2, 3, 8	6. Aerosol and cloud height using O_2 A-band
750	18		2, 5	7. Aerosol coarse mode size distribution
763	6		6	8. Cloud screening and characterization
866	52		2, 5, 8, 9	9. Surface BRF characterization
943	46		4	
1044	97	*x*	1, 3, 5, 7, 8	
1610	73		7, 8	
1886	83		4, 8	
2126	114		7, 8, 9	

3.2.3 *Multiangle imaging, areal coverage, and spatial resolution*

The MAIA camera is a four-mirror $f/5.6$ optical system with cross-track and along-track focal lengths at the center of the optical field of view of 57 and 61 mm, respectively. As the MAIA orbit is not yet known, this design accommodates any orbit altitude between 600 and 850 km. Unlike MISR, which contains multiple cameras pointed at discrete along-track view angles, MAIA's single camera is mounted on a biaxial gimbal assembly that can point the camera field of view to any along-track and cross-track position within a bidirectional field of regard. A mini dual-drive actuator (MDDA) drives each gimbal axis. The MDDA has been used on MISR and other satellite instruments, and provides each gimbal axis with 100% redundancy and resilience to single-point mechanical or electrical faults.

The targeting nature of the MAIA instrument enables routine multiangle observations of a globally distributed set of study sites. The along-track (scan) gimbal has a ± 58-deg range of motion, while the cross-track (pan) gimbal has a ± 39-deg range of motion, which when added to the ± 9-deg cross-track field of view provides a ± 48-deg cross-track field of regard. The pan capability permits access to targets that are not directly situated on the subspacecraft track, making it possible to observe each target, on average, at least three times per week. Images of the same area can be observed at a set of discrete view angles in a "step-and-stare" sequence. A "sweep" mode of operation in which the scan gimbal moves continuously over its accessible range is also possible.

For most targets, images would be acquired using the step-and-stare mode (Fig. 2). In this mode, the gimbals orient the camera to view the target's leading edge, beginning at the most oblique forward view angle. Pushbroom imagery is acquired while the camera remains fixed at this angle, after which the scan gimbal moves to the next (smaller) forward view angle and imagery of the same area is reacquired. This sequence repeats until observations are acquired at all commanded angles. The pan actuator compensates for Earth rotation between views. Observing at five view angles would yield target lengths >330 km from a 600-km orbit and >420 km from an 850-km orbit. The number of view angles is selectable, with more angles resulting in a shorter along-track distance seen in common by all views. At nadir, the camera design covers a cross-track swath width of 192 km for an orbit altitude of 600 km, increasing to 272 km at 850-km altitude. Even at the lowest altitude, the target dimensions cover major metropolitan areas. Footprint sizes are on the order of 200 m at nadir and increase with view angle, particularly in the along-track direction. At the highest orbit altitude and most oblique view angle, the along-track footprint size remains below 1100 m, and is oversampled by a factor of 4.5 as a result of the pushbroom frame rate.

3.2.4 *Instrument system*

A conceptual layout of the MAIA instrument is shown in Fig. 3. A cylindrical barrel serves as a radiator to dissipate heat from the camera electronics. Another radiator, positioned to view deep space, dissipates heat from the focal plane, which is passively cooled to 225 K to limit dark

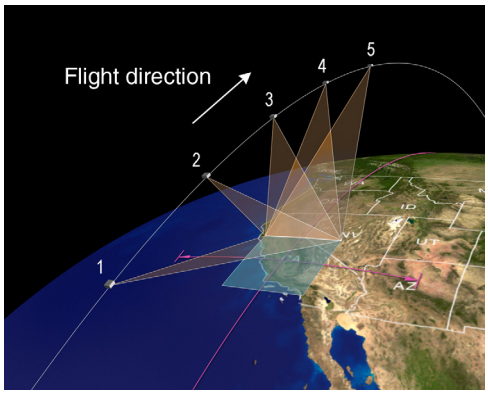

Fig. 2 Example MAIA step-and-stare sequence, showing the case of five discrete view angles.

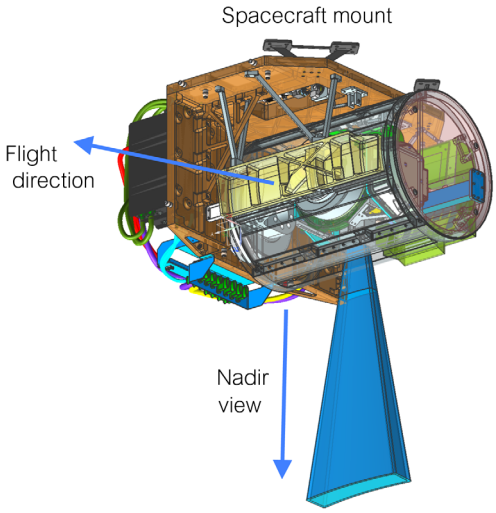

Fig. 3 Conceptual layout of the MAIA instrument.

current in the SWIR detectors. Other parts of the instrument include the structural supports, the biaxial gimbal assembly, the instrument electronics, an onboard calibrator (OBC), and a dark target (DT). The OBC consists of a glass diffuser and an array of wiregrid polarizers, and is illuminated by sunlight as the spacecraft traverses one of the orbital poles. The DT is a light-shielded cavity for measurement of dark levels. The biaxial gimbal enables periodically pointing the camera at these calibrators, and the data acquired are used in ground data processing to update the polarimetric and dark offset calibrations.

3.3 *Science Operations*

MAIA is to be launched into a low-Earth, sun-synchronous, polar orbit at an altitude in the 600- to 850-km range. The orbit altitude and mean local time of equator crossing will be established once the host spacecraft has been selected. Mid- to late-morning overpass time is preferred to allow for fog burn-off and boundary layer mixing and because fewer clouds are expected in the morning than in the afternoon.[83] In addition, because the accessible area within the instrument field of regard increases with orbit altitude, target revisit frequencies generally increase as orbit altitude increases. NASA is planning to select the host spacecraft in late 2018, and launch is expected to occur no earlier than mid-2021. The baseline mission duration is 3 years.

Science data would be collected, on average, over one target per orbit, resulting in about 100 acquisitions per week. Typical volume per target of the instrument data is estimated at 29 Gbit, slightly larger than the volume generated in one orbit by MISR, despite the fact that MAIA observes discrete targets, while MISR observes the illuminated side of the Earth continuously. This is a result of the larger number of spectral bands in MAIA, the collection of polarimetric data, and the use of onboard spatial averaging in MISR. Primary target areas (PTAs) are major population centers designated for conducting epidemiological investigations by the MAIA Science Team. PTAs would be observed in a step-and-stare mode and are selected to include major population centers covering a range of PM concentrations and particle types; surface-based aerosol sunphotometers (e.g., from AERONET[45]) for aerosol retrieval validation; PM mass, size discrimination, and chemical speciation monitors associated with various measurement networks[84,85] to enable development of statistical and machine learning regression models that relate retrieved column-integrated aerosol properties to near-surface PM; and health data geocoded by home addresses, zip codes, census block groups, or similar locations of study subjects. Secondary target areas (STAs) are regions of interest for air quality or other aerosol and cloud research (e.g., climate science) and would make use of either the step-and-stare or sweep mode, depending on the measurement objective. STAs do not have the same requirements on surface monitor availability as PTAs and the feasibility of higher-level data processing beyond generation of calibrated and georectified imagery (see § 3.4.1) would be assessed on a case-by-

case basis. Calibration/validation target areas (CVTAs) would be observed routinely for instrument calibration and stability monitoring, and aerosol/PM validation. As the MAIA instrument does not contain an absolute radiometric calibrator, the prelaunch camera calibration will be routinely updated via vicarious calibrations over Railroad Valley, Nevada. The vicarious calibration technique has been widely adopted by many satellite sensor investigations and uses surface and atmospheric measurements acquired at the time of satellite overpass to compute top-of-atmosphere radiance and to update the instrument radiometric response. MAIA observations of noninstrumented but stable Earth targets, such as the Libya-4 desert site, will also be used to maintain the radiometric calibration uncertainty to within $\pm 4\%$ over bright targets ($\pm 6\%$ over dark targets). A candidate set of PTAs, STAs, and CVTAs is shown in Fig. 4. Specialized acquisitions over targets of opportunity may be acquired over episodic events, such as volcanic eruptions, major wildfires, or dust storms.

The candidate PTAs and STAs shown in Fig. 4 include historically understudied areas (e.g., Africa). The list is subject to future updates, as observability of some targets will depend on the orbit altitude of the host spacecraft and negotiations for access to the requisite surface monitors and health data are still in process.

3.4 *Data Processing and Products*

MAIA data products follow the NASA hierarchy from level 0 (raw instrument data) to level 1 (calibrated and georectified imagery), level 2 (geophysical products at the same location as level

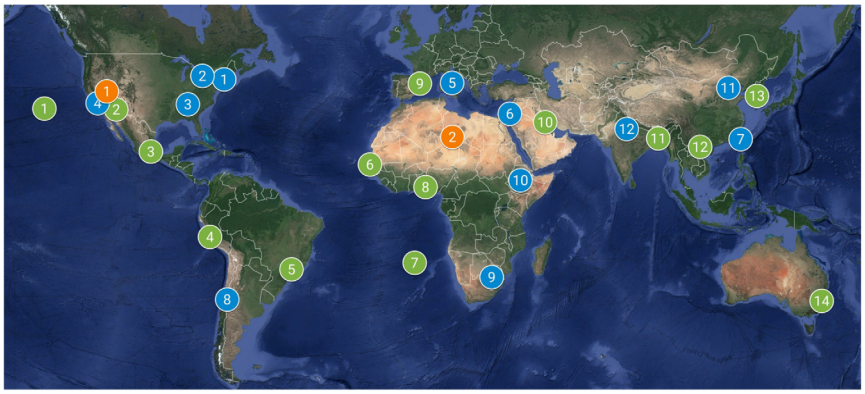

Candidate target areas — PTA — STA — CVTA

PTA		STA	
1	NE US (Boston, Providence, Hartford, New York)	1	Cloud field
2	NE Canada (Toronto, Hamilton)	2	Arizona (Phoenix)
3	SE US (Atlanta Metro)	3	Mexico (Mexico City)
4	SW US (Fresno, Bakersfield, LA, Riverside, San Bernardino)	4	Peru (Lima)
5	Italy (Rome, Bologna)	5	Brazil (São Paulo)
6	Israel (Haifa, Tel Aviv, Jerusalem, Beer Sheba)	6	Senegal (Dakar)
7	Taiwan (Taipei, New Taipei, Taichung, Tainan, Kaohsiung)	7	Cloud field
8	Chile (Santiago, Concepción)	8	Nigeria (Lagos)
9	South Africa (Johannesburg, Pretoria)	9	Spain (Barcelona)
10	Ethiopia (Addis Ababa, Adama)	10	Kuwait (Kuwait City)
11	China (Beijing)	11	Bangladesh (Dhaka)
12	India (Delhi)	12	Vietnam (Hanoi)
1	Nevada (Railroad Valley)	13	South Korea (Seoul)
2	Libya-4 desert site	14	Australia (Sydney)

Fig. 4 Candidate set of PTAs, STAs, and CVTAs and representative cities.

1 source data), and level 4 (integration of measured and modeled results). As spatial gridding and map projection are incorporated into level 1 processing in a similar manner as is done for MISR,[86] MAIA does not identify separate level 3 products. Data processing software developed at the MAIA science computing facility at JPL (with algorithmic approaches and software partially inherited from the MISR and AirMSPI projects) will be delivered to the NASA Langley ASDC for product generation.

3.4.1 *Level 1 calibrated and georectified imagery*

Level 1 calibrated and georectified radiance and polarization image products will be map-projected to the surface terrain altitude for step-and-stare acquisitions and to the surface ellipsoid for sweep observations. For those target areas that will be subjected to higher-level aerosol and PM processing, a decision tree-based algorithm capitalizing on MISR and MODIS experience[87–89] will be used operationally to detect cloud-covered pixels.

3.4.2 *Level 2 aerosol*

The level 2 MAIA aerosol processing concept is envisioned to employ a nonlinear optimization algorithm to adjust the aerosol properties to match the full set of multiangular, multispectral, and polarimetric data provided by the MAIA instrument. This algorithm has been prototyped using AirMSPI data.[90] For MAIA, acceptable limits on aerosol microphysical and optical properties would be derived by configuring the CTM regionally and analyzing the aerosol climatology for each PTA. A pre-established surface BRF database based on the Multi-Angle Implementation of Atmospheric Correction (MAIAC) algorithm[91,92] would further constrain the retrievals. Constraints on the spatial and spectral variations of aerosol properties across neighboring pixels and temporal variations of surface reflection properties[76,90] within few days of target revisits will be imposed to stabilize the algorithm. The MAIAC surface database, which has been screened for clouds, potentially adds a supplementary layer of cloud screening.[93] This approach results in retrieval of both total AOD as well as fractional AODs associated with fine, coarse, spherical, nonspherical, absorbing, and nonabsorbing aerosols on a 1-km grid. Predicted signal-to-noise ratios (SNR) in the bands used for aerosol retrievals range from approximately 190 to 880 over dark targets (worst-case surface reflectance ~0.02). Noise performance requirements have been specified to limit the effect of random instrument noise on the retrievals and to provide SNRs similar to those achieved with MISR.

3.4.3 *Level 2 PM*

The next step in the retrieval process transforms the retrieved total and fractional AODs to mass concentrations of PM_{10}, $PM_{2.5}$, and major $PM_{2.5}$ components including sulfates, nitrates, OC, BC or EC, and mineral dust. Reporting of BC or EC depends on the type of surface monitor available in a given PTA. Dust refers to resuspended inorganic material, such as soil, road dust, construction dust, or fly ash. There are several key differences between the level 2 AOD and PM products that must be accounted for in this transformation. First, AOD is a column-integrated quantity, whereas for studies of the impact of airborne PM on human health, the particles of greatest interest are near the surface. Second, PM concentrations are typically reported at controlled relative humidity (RH), whereas the MAIA AODs correspond to the ambient RH. Third, epidemiologists are interested in the average concentration of PM over a 24-h period, whereas the MAIA satellite flies over its targets at a specific time of day. Finally, the physical and optical characteristics of the particles that are captured in the AOD fields are only indirectly related to the chemical composition.

Transformations from total and fractional AOD at the time of satellite overpass to 24-h averaged total PM mass and PM species fractions, if derived solely based on MAIA observations alone, are likely to be fraught with systematic biases and uncertainties. However, previous studies have shown that geostatistical regression models (GRMs) derived from AOD, fractional AOD, and other environmental attributes, such as temperature, RH, wind speed, land cover type, and vertically resolved aerosol speciation from the CTM, along with collocated

measurements from surface monitors, can be used to empirically calibrate the satellite data at locations where surface monitors are not present and to account for the differences in how the AOD and PM products are defined.[53,94–96] An ensemble approach to GRM generation is being explored, using both a Bayesian framework as well as various machine learning methodologies, e.g., artificial neural networks, support vector machines, and random forests.[97,98]

To generate level 2 maps of speciated $PM_{2.5}$, MAIA would build upon current practice and include data from PM speciation monitors in addition to those that measure total $PM_{2.5}$ and PM_{10} in generating the GRMs. Sources of such data include the Chemical Speciation Network (CSN) and Interagency Monitoring of Protected Visual Environments (IMPROVE) network,[84] Surface PARTiculate mAtter Network (SPARTAN),[85] other existing monitors within the PTAs, and additional ground monitors to be deployed by the MAIA project. Current plans are to expand the SPARTAN network with filter-based samplers in the MAIA PTAs. To deal with the several-month latency associated with the availability of CSN, IMPROVE, and SPARTAN data, monthly averaged species fractions from the same month in previous years, supplemented by ancillary information, such as temperature and RH, will be used to generate interim estimates of speciated $PM_{2.5}$ at the monitor locations. Once the actual data become available, MAIA level 2 products will be reprocessed.

Deployment of low-cost light-scattering-based particle sensors such as PurpleAir (PA)[99] is also under consideration to supplement existing government-sponsored $PM_{2.5}$ and PM_{10} networks. Field and laboratory tests conducted by the South Coast Air Quality Management District's (SCAQMD) Air Quality Sensor Performance Evaluation Center (AQ-SPEC) indicate that while the PA tends to overestimate PM mass, a high degree of correlation with EPA's reference methods is found,[100] enabling correction for systematic biases in the PA data. JPL has deployed several PA sensors (on loan from SCAQMD) in Bakersfield, Fresno, and Visalia, California for further evaluation.

3.4.4 *Level 4 gap-filled PM*

The level 2 PM maps are populated with data only where cloud-screened aerosol retrievals using MAIA instrument data have been generated. Furthermore, level 2 maps are not generated on days for which there are no satellite overpasses. To generate the spatially and temporally gap-filled PM exposure estimates that are needed for the epidemiological investigations, the MAIA project plans to produce a daily gap-filled level 4 PM product in which spatial gaps due to cloud cover or other dropout are filled and PM estimates are generated on nonoverpass days. Three sources of data serve as input to generation of this product: the level 2 instrument-based PM product, interpolated maps generated from surface monitor measurements, and PM mass and species fractional concentrations predicted by a CTM. Complete spatial and temporal coverage for each PTA would be obtained by fusing the satellite retrievals, ground-level concentration measurements, and CTM outputs in postretrieval processing.

The level 4 PM estimates are envisioned to be weighted averages determined by the relative predictive ability of each input source. The weights may vary across space and time, and are derived from uncertainty estimates associated with each of the inputs. Uncertainties associated with the level 2 satellite-based product would be generated as part of the retrieval algorithm. Interpolated values from surface monitors will be most accurate for locations and times closest to the monitor position and sampling period, and high uncertainties would be assigned where geographical factors, such as surface elevation changes, would make the interpolations unreliable. For the CTM, MAIA plans to use the mesoscale Weather Research and Forecasting model coupled with chemistry (WRF-Chem) model,[101,102] coupled with wildfire smoke emissions from the Fire Locating and Modeling of Burning Emissions system[103] and nested within the GEOS-Chem global model of atmospheric composition driven by meteorological observations from the Goddard Earth Observing System.[104] WRF-Chem outputs will be generated on a 4-km grid and GEOS-Chem on a 25-km grid. To account for biases that are known to plague even state-of-the-art CTMs,[105] WRF-Chem outputs will be improved throughout the mission using model output statistics that are analyzed through comparison with MAIA level 2 speciated PM maps and data from surface monitors. For example, a recent study[106] calibrated GEOS-Chem outputs using speciation monitoring data combined with meteorological and land use variables using

a backward propagation neural network, which allows for complex and nonlinear associations between model inputs. This model was used to predict daily $PM_{2.5}$ and constituents mass concentrations on a downscaled 1-km grid. Accuracy of the predictions was assessed using k-fold cross validation. The mean total R^2 at left out monitors was 0.85, 0.71, 0.69, 0.83, and 0.81 for $PM_{2.5}$, EC, OC, nitrate, and sulfate, respectively.

As with MISR, archiving and distribution of MAIA data products will be the responsibility of the ASDC. To protect individual privacy, none of the publicly available geophysical data products generated by the MAIA investigation and stored at the ASDC will contain any health data. Health records accessed by epidemiologists and public health experts on the MAIA team will be handled in accordance with well-established legal and ethical requirements for confidentiality, privacy protection, and data security.

3.5 *Science Investigation*

Various epidemiological studies are planned for the different MAIA PTAs depending on the predominant PM species present, the type of health records available, and previous studies of the effects of air pollution in each area. Well-established epidemiological methodologies, such as time-series, case-crossover, and cohort-study designs[107–109] will be used.

Information about the candidate set of PTAs (see Fig. 4) is shown in Table 2. The MAIA science team plans to focus on health effects associated with a range of PM concentrations and different time scales of exposure. Acute exposure takes place over a period of several days and is generally associated with premature mortality and increased hospital visits due to both cardiovascular and respiratory diseases. These studies are conducted by analyzing vital statistics records (e.g., death certificates) and records of hospital admissions or emergency room visits. Subchronic exposure studies are primarily aimed at birth outcomes and pregnancy complications, such as low birth weight and preeclampsia. These outcomes are usually investigated by analyzing birth records contained in an area's vital statistics data, or by establishing a birth cohort. Chronic exposure studies usually track individual-level health effects over multiple years, and are important as they document morbidity and mortality risk increases and are often used in GBD estimates. These are generally done with an established cohort or by analyzing existing health records combined with long-term residency data.[111]

Table 2 Characteristics of the candidate PTAs.

Candidate PTA	Representative PM2.5 concentration[110] ($\mu g\,m^{-3}$)	Study type		
		Acute	Subchronic	Chronic
Northeast US	9	x	x	x
Northeast Canada	9			x
Southeast US	13	x		
Southwest US	17	x	x	
Italy	17	x		x
Israel	20	x	x	x
Taiwan	26		x	
Chile	27	x	x	
South Africa	46	x		
Ethiopia	70		x	x
China	80	x		x
India	118	x		

As noted earlier, the baseline MAIA mission is 3 years in duration. Many epidemiological studies conducted around the world have reported associations between acute (daily) PM exposure and mortality, hospital admissions, and emergency department visits using <3 years of data in densely populated regions.[112–115] Adverse impacts on prenatal or neonatal development, e.g., restricted intrauterine growth, preterm delivery, low birth weight, congenital heart defects, and infant mortality,[5,116,117] have been associated with PM exposure during specific pregnancy trimesters.[118,119] Hence, investigations into birth outcomes targeting trimester specific effects can even utilize <1 year of data if the population of pregnant women residing in the area is large enough.[120–122] Long-term studies relating chronic exposure to cardiovascular disease have also benefited from only 2 to 3 years of data, and several have obtained statistically significant results using only a single year.[65,123–128] Although this may seem surprising, PM spatial patterns and the rank order tend to be fairly stable from year to year, and results show that the inferred health impacts from shorter-term exposures are consistent with studies using longer exposure periods.[65] These epidemiological studies targeting chronic health outcomes typically make use of large cohorts (groups of people, who have been exposed to air pollutants at different levels or compositions over long periods of time).

Health studies with geocoded subject locations at high spatial resolution (address level) enable the most accurate estimation of PM exposure-related health effects. MAIA's resolution enables PM retrievals on a 1-km grid for sampling within the neighborhood scale. Although sulfate has relatively low spatial variability at urban-to-regional scales,[129] nitrate and primary OC vary over smaller spatial scales. BC aerosols are very heterogeneous due to their generation from traffic fuel combustion and biomass burning.[129,130] Recent research highlights the value of 1-km satellite-based aerosol data for health effect studies.[96,131–133]

4 Conclusions

Building upon the success of MISR and other satellite instruments in providing aerosol observations that have contributed to numerous health studies, the MAIA investigation aims to take these efforts further by delving more deeply into assessing the contributions of different types of airborne particles to human health. Although much of the development effort is concerned with design and fabrication of the satellite instrument, the investigation also heavily relies on surface monitors and the CTM to generate PM maps needed to carry out the mission objectives. Although PM monitoring for regulatory purposes is largely concerned with absolute particle mass concentrations, epidemiological studies focus on the response associated with relative differences in exposure to ambient PM. Consequently, the MAIA data processing approach is designed at each step to eliminate systematic biases in the PM products, beginning with calibration of the instrument imagery, validation of the column AOD products, application of empirically derived GRMs to transform AOD to PM, and use of satellite and surface observations to remove biases in the CTM that provides a key element of the gap-filling strategy. The impact of random errors is mitigated by the statistical advantage of observing entire major metropolitan areas from space, and acquiring health information associated with hundreds of thousands to millions of individuals. With the inclusion of epidemiologists on the science team, MAIA is the first competitively selected NASA satellite mission with applications/societal benefits as its primary objective.

Disclosures

The authors declare that there are no conflicts of interest.

Acknowledgments

The authors acknowledge the participation of a multidisciplinary team in the MAIA investigation, including experts in system engineering, instrument design and fabrication, project and resource management, data systems, instrument operations, aerosol and cloud remote sensing, epidemiology, and public health. Specific mention is given to our collaborators Bert Brunekreef

(Utrecht University), Sagnik Dey (IIT Delhi), Kembra Howdeshell (National Institute of Environmental Health Sciences), John Langstaff (EPA), Pius Lee (National Oceanic and Atmospheric Administration), and Fuyuen Yip (Centers for Disease Control and Prevention), as well as many local personnel in the various PTAs who will assist with various aspects of the project. This paper represents the current development status of the MAIA investigation. The decision to implement MAIA will not be finalized until NASA completes the National Environmental Policy Act (NEPA) process. This research is carried out, in part, at the Jet Propulsion Laboratory, California Institute of Technology, under contract with the National Aeronautics and Space Administration (NASA). The data in Fig. 1 were obtained from the NASA Langley Research Center Atmospheric Science Data Center.

References

1. C. A. Pope, III and D. W. Dockery, "Health effects of fine particulate air pollution: lines that connect," *J. Air Waste Manag. Assoc.* **56**, 709–742 (2006).
2. R. D. Brook et al., "Particulate matter air pollution and cardiovascular disease: an update to the scientific statement from the American Heart Association," *Circulation* **121**, 2331–2378 (2010).
3. C. A. Pope, III et al., "Lung cancer, cardiopulmonary mortality, and long-term exposure to fine particulate air pollution," *JAMA* **287**, 1132–1141 (2002).
4. J. S. Apte et al., "Addressing global mortality from ambient PM2.5," *Environ. Sci. Technol.* **49**(13), 8057–8066 (2015).
5. B. Ritz and M. Wilmhelm, "Ambient air pollution and adverse birth outcomes: methodologic issues in an emerging field," *Basic Clin. Pharmacol. Toxicol.* **102**, 182–190 (2008).
6. GBD 2016 Risk Factors Collaborators, "Global, regional, and national comparative risk assessment of 84 behavioural, environmental and occupational, and metabolic risks or clusters of risks, 1990-2016: a systematic analysis for the Global Burden of Disease Study 2016," *Lancet* **390**, 1345–1422 (2017).
7. M. Brauer et al., "Ambient air pollution exposure estimation for the Global Burden of Disease 2013," *Environ. Sci. Technol.* **50**, 79–88 (2016).
8. A. J. Cohen et al., "Estimates and 25-year trends of the global burden of disease attributable to ambient air pollution: an analysis of data from the Global Burden of Diseases Study 2015," *Lancet* **389**, 1907–1918 (2017).
9. M. L. Bell et al., "Spatial and temporal variation in $PM_{2.5}$ chemical composition in the United States for health effects studies," *Environ. Health Perspect.* **115**, 989–995 (2007).
10. US Environmental Protection Agency, "National ambient air quality standards for particulate matter; final rule," Federal Register 78, No. 10 (2013).
11. World Bank, "Air Pollution in World Cities (PM10 Concentrations)," http://microdata.worldbank.org/index.php/catalog/424 (2012).
12. National Research Council, National Academy of Sciences, "Research priorities for airborne particulate matter: IV. Continuing research progress," Washington, D.C., http://www.nap.edu/catalog.php?record_id=10957 (2004).
13. Z. Ross et al., "Spatial and temporal estimation of air pollutants in New York City: exposure assignment for use in a birth outcomes study," *Environ. Health* **12**, 51–63 (2013).
14. M. Franklin et al., "Characterization of subgrid-scale variability in particulate matter with respect to satellite aerosol observations," *Remote Sens.* **10**, 623 (2018).
15. K. de Hoogh et al., "Modelling daily PM2.5 concentrations at high spatio-temporal resolution across Switzerland," *Environ. Pollut.* **233**, 1147–1154 (2018).
16. US Environmental Protection Agency, *Quality Assurance Handbook for Air Pollution Measurement Systems*, Vol. II, Ambient Air Quality Monitoring Program, EPA-454/B-13-003 (2013).
17. S. Tinkle et al., "Integrated earth observations: application to air quality and human health," Report of a workshop sponsored by the National Institute of Environmental Health Sciences (NIEHS) and the US Environmental Protection Agency, https://nepis.epa.gov/Exe/ZyPURL.cgi?Dockey=P1002ZV0.TXT (2007).

18. I. Kloog et al., "Long- and short-term exposure to PM2.5 and mortality: using novel exposure models," *Epidemiology* **24**, 555–561 (2013).
19. D. L. Crouse et al., "Risk of nonaccidental and cardiovascular mortality in relation to long-term exposure to low concentrations of fine particulate matter: a Canadian national-level cohort study," *Environ. Health Perspect.* **120**, 708–714 (2012).
20. National Academies of Sciences, Engineering, and Medicine, *Thriving on Our Changing Planet: A Decadal Strategy for Earth Observation from Space*, The National Academies Press, Washington, DC (2018).
21. J. V. Martonchik, D. J. Diner, and R. A. Kahn, "Retrieval of aerosol properties over land using MISR observations," in *Satellite Aerosol Remote Sensing over Land*, A. Kokhanovsky, Ed., pp. 267–293, Springer Praxis Books, Berlin, Germany (2009).
22. R. C. Levy et al., "The collection 6 MODIS aerosol products over land and ocean," *Atmos. Meas. Tech.* **6**, 2989–3034 (2013).
23. A. M. Sayer et al., "Global and regional evaluation of over-land spectral aerosol optical depth retrievals from SeaWiFS," *Atmos. Meas. Tech.* **5**, 1761–1778 (2012).
24. B. L. Boys et al., "Fifteen-year global time series of satellite-derived fine particulate matter," *Environ. Sci. Technol.* **48**, 11109–11118 (2014).
25. A. van Donkelaar et al., "Use of satellite observations for long-term exposure assessment of global concentrations of fine particulate matter," *Environ. Health Perspect.* **123**, 135–143 (2016).
26. H. Lin et al., "Consumption of fruit and vegetables might mitigate the adverse effects of ambient PM2.5 on lung function among adults," *Environ. Res.* **160**, 77–82 (2018).
27. B. Bowe et al., "Particulate matter air pollution and the risk of incident CKD and progression to ESRD," *J. Am. Soc. Nephrol.* **29**, 218–230 (2018).
28. Y. Guo et al., "The burden of lung cancer mortality attributable to fine particles in China," *Sci. Total Environ.* **579**, 1460–1466 (2017).
29. G. Tagliabue et al., "Atmospheric fine particulate matter and breast cancer mortality: a population-based cohort study," *BMJ Open* **6**, e012580 (2016).
30. H. Chen et al., "Ambient fine particulate matter and mortality among survivors of myocardial infarction: population-based cohort study," *Environ. Health Perspect.* **124**(9), 1421–1428 (2016).
31. H. Chen et al., "Risk of incident diabetes in relation to long-term exposure to fine particulate matter in Ontario, Canada," *Environ. Health Perspect.* **121**(7), 804–810 (2013).
32. N. L. Fleischer et al., "Outdoor air pollution, preterm birth, and low birth weight: analysis of the World Health Organization Global Survey on Maternal and Perinatal Health," *Environ. Health Perspect.* **122**, 425–430 (2014).
33. D. J. Diner et al., "Multi-angle Imaging SpectroRadiometer (MISR) instrument description and experiment overview," *IEEE Trans. Geosci. Rem. Sens.* **36**, 1072–1087 (1998).
34. P.-Y. Deschamps et al., "The POLDER mission: instrument characteristics and scientific objectives," *IEEE Trans. Geosci. Remote Sens.* **32**, 598–615 (1994).
35. R. A. Kahn and B. J. Gaitley, "An analysis of global aerosol type as retrieved by MISR," *J. Geophys. Res.-Atmos.* **120**, 4248–4281 (2015).
36. D. Tanré et al., "Remote sensing of aerosols by using polarized, directional and spectral measurements within the A-Train: the PARASOL mission," *Atmos. Meas. Tech.* **4**, 1383–1395 (2011).
37. Y. Liu and D. J. Diner, "Multi-Angle Imager for Aerosols: a satellite investigation to benefit public health," *Publ. Health Rep.* **132**, 14–17 (2017).
38. https://eosweb.larc.nasa.gov/project/misr/misr_table.
39. https://misr.jpl.nasa.gov/publications/peerReviewed/.
40. D. J. Diner et al., "The value of multiangle measurements for retrieving structurally and radiatively consistent properties of clouds, aerosols, and surfaces," *Remote Sens. Environ.* **97**, 495–518 (2005).
41. O. V. Kalashnikova et al., "Ability of multi-angle remote sensing observations to identify and distinguish mineral dust types: optical models and retrievals of optically thick plumes," *J. Geophys. Res.-Atmos.* **110**, D18S14 (2005).

42. O. V. Kalashnikova et al., "MISR dark water aerosol retrievals: operational algorithm sensitivity to particle non-sphericity," *Atmos. Meas. Tech.* **6**, 2131–2154 (2013).
43. J. V. Martonchik et al., "Techniques for the retrieval of aerosol properties over land and ocean using multiangle imaging," *IEEE Trans. Geosci. Remote Sens.* **36**, 1212–1227 (1998).
44. D. J. Diner et al., "Using angular and spectral shape similarity constraints to improve MISR aerosol and surface retrievals over land," *Remote Sens. Environ.* **94**, 155–171 (2005).
45. B. N. Holben et al., "AERONET—a federated instrument network and data archive for aerosol characterization," *Remote Sens. Environ.* **66**, 1–16 (1998).
46. W. A. Abdou et al., "Comparison of coincident MISR and MODIS aerosol optical depths over land and ocean scenes containing AERONET sites," *J. Geophys. Res.-Atmos.* **110**, D10S07 (2005).
47. R. A. Kahn et al., "Multiangle Imaging SpectroRadiometer global aerosol product assessment by comparison with the Aerosol Robotic Network," *J. Geophys. Res.-Atmos.* **115**, D23209 (2010).
48. J. V. Martonchik et al., "Comparison of MISR and AERONET aerosol optical depths over desert sites," *Geophys. Res. Lett.* **31**, L16102 (2004).
49. X. Jiang et al., "Comparison of MISR aerosol optical thickness with AERONET measurements in Beijing metropolitan area," *Remote Sens. Environ.* **107**, 45–53 (2007).
50. Y. Liu et al., "Validation of Multiangle Imaging SpectroRadiometer (MISR) aerosol optical thickness measurements using Aerosol Robotic Network (AERONET) observations over the contiguous United States," *J. Geophys. Res.-Atmos.* **109**, D06205 (2004).
51. A. van Donkelaar et al., "Global estimates of fine particulate matter using a combined geophysical-statistical method with information from satellites, models, and monitors," *Environ. Sci. Technol.* **50**, 3762–3772 (2016).
52. Y. Liu, R. Kahn, and P. Koutrakis, "Estimating PM2.5 component concentrations and size distributions using satellite retrieved fractional aerosol optical depth: part 1—method development," *J. Air Waste Manag. Assoc.* **57**, 1351–1359 (2007).
53. Y. Liu et al., "Estimating PM2.5 component concentrations and size distributions using satellite retrieved fractional aerosol optical depth: part 2—a case study," *J. Air Waste Manag. Assoc.* **57**, 1360–1369 (2007).
54. Y. Liu, B. A. Schichtel, and P. Koutrakis, "Estimating particle sulfate concentrations using MISR retrieved aerosol properties," *IEEE J. Sel. Top. Appl. Earth Obs. Remote Sens.* **2**, 176–184 (2009).
55. S. Dey and L. Di Girolamo, "A decade of change in aerosol properties over the Indian subcontinent," *Geophys. Res. Lett.* **38**, L14811 (2011).
56. S. Dey et al., "Variability of outdoor fine particulate (PM2.5) concentration in the Indian Subcontinent: a remote sensing approach," *Remote Sens. Environ.* **127**, 153–161 (2012).
57. Y. Q. Wang et al., "A hierarchical Bayesian approach for aerosol retrieval using MISR data," *J. Am. Stat. Assoc.* **108**, 483–493 (2013).
58. T. Moon et al., "Evaluation of a MISR-based high-resolution aerosol retrieval method using AERONET DRAGON campaign data," *IEEE Trans. Geosci. Remote Sens.* **53**, 4328–4339 (2015).
59. M. J. Garay, O. V. Kalashnikova, and M. A. Bull, "Development and assessment of a higher-spatial-resolution (4.4 km) MISR aerosol optical depth product using AERONET-DRAGON data," *Atmos. Chem. Phys.* **17**, 5095–5106 (2017).
60. M. Franklin, O. V. Kalashnikova, and M. J. Garay, "Size-resolved particulate matter concentrations derived from 4.4 km-resolution size-fractionated Multi-angle Imaging SpectroRadiometer (MISR) aerosol optical depth over Southern California," *Remote Sens. Environ.* **196**, 312–323 (2017).
61. X. Meng et al., "Estimating $PM_{2.5}$ speciation concentrations using prototype 4.4 km-resolution MISR aerosol properties over Southern California," *Atmos. Environ.* **181**, 70–81 (2018).
62. T. P. Ackerman et al., "Integrating and interpreting aerosol observations and models within the PARAGON framework," *Bull. Am. Meteorol. Soc.* **85**, 1523–1533 (2004).

63. M. L. Bell et al., "Prenatal exposure to fine particulate matter and birth weight: variations by particulate constituents and sources," *Epidemiology* **21**, 884–891 (2010).
64. M. Franklin, P. Koutrakis, and J. Schwartz, "The role of particle composition on the association between $PM_{2.5}$ and mortality," *Epidemiology* **19**, 680–689 (2008).
65. B. Ostro et al., "Long-term exposure to constituents of fine particulate air pollution and mortality: results from the California Teachers Study," *Environ. Health Perspect.* **118**, 363–369 (2010).
66. R. D. Peng et al., "Emergency admissions for cardiovascular and respiratory diseases and the chemical composition of fine particle air pollution," *Environ. Health Perspect.* **117**, 957–963 (2009).
67. J. A. Sarnat et al., "Fine particle sources and cardiorespiratory morbidity: an application of chemical mass balance and factor analytical source-apportionment methods," *Environ. Health Perspect.* **116**, 459–466 (2008).
68. M. Z. Jacobson, *Atmospheric Pollution: History, Science, and Regulation*, Cambridge University Press, United Kingdom (2002).
69. H. Jethva and O. Torres, "Satellite-based evidence of wavelength-dependent aerosol absorption in biomass burning smoke inferred from Ozone Monitoring Instrument," *Atmos. Chem. Phys.* **11**, 10541–10551 (2009).
70. L. Wu et al., "Aerosol retrieval from multiangle multispectral photopolarimetric measurements: importance of spectral range and angular resolution," *Atmos. Meas. Tech.* **8**, 2625–2638 (2015).
71. B. Cairns et al., "Polarimetric remote sensing of aerosols over land surfaces," in *Satellite Aerosol Remote Sensing over Land*, A. Kokhanovsky, Ed., pp. 295–323, Springer Praxis Books, Berlin, Germany (2009).
72. P. Dubuisson et al., "Estimating the altitude of aerosol plumes over the ocean from reflectance ratio measurements in the O_2 A-band," *Remote Sens. Environ.* **113**, 1899–1911 (2009).
73. N. Ferlay et al., "Toward new inferences about cloud structures from multidirectional measurements in the oxygen A band: middle-of-cloud pressure and cloud geometrical thickness from POLDER-3/PARASOL," *J. Appl. Meteorol. Climatol.* **49**, 2492–2507 (2010).
74. O. P. Hasekamp and J. Landgraf, "Retrieval of aerosol properties over land surfaces: capabilities of multiple-viewing-angle intensity and polarization measurements," *Appl. Opt.* **46**, 3332–3344 (2007).
75. F. Waquet et al., "Polarimetric remote sensing of aerosols over land," *J. Geophys. Res.-Atmos.* **114**, D01206 (2009).
76. O. Dubovik et al., "Statistically optimized inversion algorithm for enhanced retrieval of aerosol properties from spectral multi-angle polarimetric satellite observations," *Atmos. Meas. Tech.* **4**, 975–1018 (2011).
77. O. V. Kalashnikova et al., "Photopolarimetric sensitivity to black carbon content of wildfire smoke: Results from the 2016 ImPACT-PM field campaign," *J. Geophys. Res.-Atmos.* **123**, 5376–5396 (2018).
78. Aerosol-Cloud-Ecosystems (ACE) Study Team, "ACE 2011–2015 progress report and future outlook," https://acemission.gsfc.nasa.gov/documents/ACE_5YWP-FINAL_Redacted.pdf (2016).
79. D. J. Diner et al., "Dual photoelastic modulator-based polarimetric imaging concept for aerosol remote sensing," *Appl. Opt.* **46**, 8428–8445 (2007).
80. D. J. Diner et al., "First results from a dual photoelastic-modulator-based polarimetric camera," *Appl. Opt.* **49**, 2929–2946 (2010).
81. D. J. Diner et al., "The Airborne Multiangle SpectroPolarimetric Imager (AirMSPI): a new tool for aerosol and cloud remote sensing," *Atmos. Meas. Tech.* **6**, 2007–2025 (2013).
82. D. J. Diner et al., "Application of the first and second generation airborne multiangle spectropolarimetric imagers (AirMSPI and AirMSPI-2) to cloud and aerosol remote sensing," 2014, https://ams.confex.com/ams/14CLOUD14ATRAD/webprogram/Paper250571.html.
83. R. Eastman and S. G. Warren, "Diurnal cycles of cumulus, cumulonimbus, stratus, stratocumulus, and for from surface observations over land and ocean," *J. Clim.* **27**, 2386–2404 (2014).

84. P. A. Solomon et al., "U.S. National $PM_{2.5}$ chemical speciation monitoring networks—CSN and IMPROVE: description of networks," *J. Air Waste Manag. Assoc.* **64**, 1410–1438 (2014).
85. G. Snider et al., "SPARTAN: a global network to evaluate and enhance satellite-based estimates of ground-level particulate matter for global health applications," *Atmos. Meas. Tech.* **8**, 505–521 (2015).
86. G. W. Bothwell et al., "The Multi-angle Imaging SpectroRadiometer science data system, its products, tools and performance," *IEEE Trans. Geosci. Remote Sens.* **40**, 1467–1147 (2002).
87. S. A. Ackerman et al., "Discriminating clear sky from clouds with MODIS," *J. Geophys. Res.-Atmos.* **103**, 32141–32158 (1998).
88. G. Zhao and L. Di Girolamo, "A cloud fraction versus view angle technique for automatic in-scene evaluation of the MISR cloud mask," *J. Appl. Meteor.* **43**, 860–869 (2004).
89. Y. Yang, L. Di Girolamo, and D. Mazzoni, "Selection of the automated thresholding algorithm for the Multi-angle Imaging SpectroRadiometer radiometric camera-by-camera cloud mask," *Remote Sens. Environ.* **107**, 159–171 (2007).
90. F. Xu et al., "Coupled retrieval of aerosol properties and land surface reflection using the Airborne Multiangle SpectroPolarimetric Imager (AirMSPI)," *J. Geophys. Res.-Atmos.* **122**, 7004–7026 (2017).
91. A. Lyapustin et al., "Multiangle implementation of atmospheric correction (MAIAC): 1. Radiative transfer basis and look-up tables," *J. Geophys. Res.-Atmos.* **116**, D03210 (2011).
92. A. Lyapustin et al., "Multiangle implementation of atmospheric correction (MAIAC): 2. Aerosol algorithm," *J. Geophys. Res.-Atmos.* **116**, D03211 (2011).
93. A. Lyapustin et al., "Improved cloud screening in MAIAC aerosol retrievals using spectral and spatial analysis," *Atmos. Meas. Tech.* **5**, 843–850 (2012).
94. I. Kloog et al., "Incorporating local land use regression and satellite aerosol optical depth in a hybrid model of spatiotemporal PM2.5 exposures in the mid-Atlantic states," *Environ. Sci. Technol.* **46**, 11913–11921 (2012).
95. X. Hu et al., "Estimating ground-level PM2.5 concentrations in the Southeastern United States using MAIAC AOD retrievals and a two-stage model," *Remote Sens. Environ.* **140**, 220–232 (2014).
96. X. Hu et al., "10-year spatial and temporal trends of PM2.5 concentrations in the Southeastern US estimated using high-resolution satellite data," *Atmos. Chem. Phys.* **14**, 6301–6314 (2014).
97. X. Hu et al., "Estimating PM2.5 concentrations in the conterminous United States using the random forest approach," *Environ. Sci. Technol.* **51**, 6936–6944 (2017).
98. H. H. Chang, X. Hu, and Y. Liu, "Calibrating MODIS aerosol optical depth for predicting daily PM2.5 concentrations via statistical downscaling," *J. Expos. Sci. Environ. Epidemiol.* **24**, 398–404 (2013).
99. K. E. Kelly et al., "Ambient and laboratory evaluation of a low-cost particulate matter sensor," *Environ. Pollut.* **221**, 491–500 (2017).
100. South Coast Air Quality Management District, Air Quality Sensor Performance Evaluation Center, "Field evaluation: Purple Air (PA-II) PM sensor," http://www.aqmd.gov/docs/default-source/aq-spec/field-evaluations/purple-air-pa-ii---field-evaluation.pdf?sfvrsn=4 (7 July 2018).
101. J. D. Fast et al., "Evolution of ozone, particulates, and aerosol direct forcing in an urban area using a new fully-coupled meteorology, chemistry, and aerosol model," *J. Geophys. Res.-Atmos.* **111**, D21305 (2006).
102. L. Wu et al., "WRF-Chem simulation of aerosol seasonal variability in the San Joaquin Valley," *Atmos. Chem. Phys.* **17**, 7291–7309 (2017).
103. J. S. Reid et al., "Global monitoring and forecasting of biomass-burning smoke: description and lessons from the fire locating and modeling of burning emissions (FLAMBE) program," *IEEE J. Sel. Topics Appl. Earth Observ. Remote Sens.* **2**, 144–162 (2009).
104. I. Bey et al., "Global modeling of tropospheric chemistry with assimilated meteorology: model description and evaluation," *J. Geophys. Res.-Atmos.* **106**, 23073–23095 (2001).

105. Y. Zhang et al., "Probing into regional ozone and particulate matter pollution in the United States: 1. A 1 year CMAQ simulation and evaluation using surface and satellite data," *J. Geophys. Res.-Atmos.* **114**, D22304 (2009).
106. Q. Di et al., "Assessing PM2.5 exposures with high spatiotemporal resolution across the continental United States," *Environ. Sci. Technol.* **50**, 4712–4721 (2016).
107. C. J. Mann, "Observational research methods. Research design II: cohort, cross sectional, and case-control studies," *Emerg. Med. J.* **20**, 54–60 (2003).
108. D. Levy et al., "Referent selection in case-crossover analyses of acute health effects of air pollution," *Epidemiology* **12**, 186–192 (2001).
109. K. J. Rothman, S. Greenland, and T. L. Lash, *Modern Epidemiology*, 3rd ed., Lippincott Williams & Wilkins, Philadelphia, PA (2008).
110. http://www.who.int/phe/health_topics/outdoorair/databases/cities/en/ (2016), https://www.epa.gov/outdoor-air-quality-data/air-quality-statistics-report (2016), or private communications from local collaborators.
111. D. L. Crouse et al., "Risk of nonaccidental and cardiovascular mortality in relation to long-term exposure to low concentrations of fine particulate matter: a Canadian national-level cohort study," *Environ. Health Perspect.* **120**, 708–714 (2012).
112. F. Forastiere et al., "A case-crossover analysis of out-of-hospital coronary deaths and air pollution in Rome, Italy," *Am. J. Respir. Crit. Care Med.* **172**, 1549–1555 (2005).
113. H. Kan and B. Chen, "A case-crossover analysis of air pollution and daily mortality in Shanghai," *J. Occup. Health* **45**, 119–124 (2003).
114. T. F. Mar et al., "PM source apportionment and health effects. 3. Investigation of inter-method variations in associations between estimated source contributions of PM2.5 and daily mortality in Phoenix, AZ," *J. Exposure Sci. Environ. Epidemiol.* **16**, 311–320 (2005).
115. B. Ostro et al., "Fine particulate air pollution in nine California counties: results from CALFINE," *Environ. Health Perspect.* **114**, 29–33 (2006).
116. S. M. Gilboa et al., "Relation between ambient air quality and selected birth defects, Seven County Study, Texas, 1997–2000," *Am. J. Epidemiol.* **162**, 238–252 (2005).
117. R. J. Šrám et al., "Ambient air pollution and pregnancy outcomes: a review," *Environ. Health Perspect.* **113**, 375–382 (2005).
118. Y.-J. Suh et al., "Cytochrome P450IA1 polymorphisms along with PM10 exposure contribute to the risk of birth weight reduction," *Reproduct. Toxicol.* **24**, 281–288 (2007).
119. E. H. van den Hooven et al., "Air pollution exposure during pregnancy, ultrasound measures of fetal growth, and adverse birth outcomes: a prospective cohort study," *Environ. Health Perspect.* **120**, 150–156 (2012).
120. N. Gouveia, S. A. Bremner, and H. M. D. Novaes, "Association between ambient air pollution and birth weight in São Paulo, Brazil," *J. Epidemiol. Commun. Health* **58**, 11–17 (2004).
121. J. D. Parker et al., "Air pollution and birth weight among term infants in California," *Pediatrics* **115**, 121–128 (2005).
122. B. Ritz et al., "Ambient air pollution and preterm birth in the environment and pregnancy outcomes study at the University of California, Los Angeles," *Am. J. Epidemiol.* **166**, 1045–1052 (2007).
123. B. Hoffman et al., "Chronic residential exposure to particulate matter air pollution and systemic inflammatory markers," *Environ. Health Perspect.* **117**, 1302–1308 (2009).
124. M. Jerrett et al., "Particulate air pollution, social confounders, and mortality in small areas of an industrial city," *Social Sci. Med.* **60**, 2845–2863 (2005).
125. M. Jerrett et al., "Spatial analysis of air pollution and mortality in Los Angeles," *Epidemiol.* **16**, 727–736 (2005).
126. N. Künzli et al., "Ambient air pollution and atherosclerosis in Los Angeles," *Environ. Health Perspect.* **113**, 201–206 (2005).
127. K. A. Miller et al., "Long-term exposure to air pollution and incidence of cardiovascular events in women," *New. Engl. J. Med.* **356**, 447–458 (2007).
128. R. C. Puett et al., "Chronic particulate exposure, mortality, and coronary heart disease in the Nurses' Health Study," *Am. J. Epidemiol.* **168**, 1161–1168 (2008).

129. A. Gryparis et al., "Measurement error caused by spatial misalignment in environmental epidemiology," *Biostatistics* **10**, 258–274 (2009).
130. Y. Zhou and J. Levy, "Factors influencing the spatial extent of mobile source air pollution impacts: a meta-analysis," *BMC Public Health* **7**, 89 (2007).
131. A. A. Chudnovsky et al., "Fine particulate matter predictions using high resolution aerosol optical depth (AOD) retrievals," *Atmos. Environ.* **89**, 189–198 (2014).
132. I. Kloog et al., "A new hybrid spatio-temporal model for estimating daily multi-year PM2.5 concentrations across northeastern USA using high resolution aerosol optical depth data," *Atmos. Environ.* **95**, 581–590 (2014).
133. L. L. Pinault et al., "Associations between fine particulate matter and mortality in the 2001 Canadian Census Health and Environment Cohort," *Environ. Res.* **159**, 406–415 (2017).

David J. Diner is a senior research scientist at the Jet Propulsion Laboratory, California Institute of Technology. He received his BS degree in physics from the State University of New York at Stony Brook and his MS and PhD degrees in planetary science from Caltech. He is the principal investigator of MISR, AirMSPI, AirMSPI-2, and MAIA. His research interests include atmospheric optics, remote sensing instrument development, and aerosol impacts on air quality and climate.

Stacey W. Boland is the project systems engineer for MAIA at JPL. She received her BS degree in physics from the University of Texas at Dallas and her MS and PhD degrees in mechanical engineering from Caltech. She has led numerous mission and instrument concept studies, and is a member of the Steering Committee for the 2017 Decadal Survey for Earth Science and Applications from Space.

Michael Brauer is a professor in the School of Population Health at the University of British Columbia and an affiliate professor at the Institute for Health Metrics and Evaluation at the University of Washington. He received his BA degrees in biochemistry and environmental science from UC-Berkeley and his ScD degree in environmental health from Harvard. He is an advisor to the World Health Organization and a member of the Core Analytic Team for the Global Burden of Disease.

Carol Bruegge is a member of the technical staff at JPL specializing in instrument calibration. She received her BA and MS degrees in applied physics from the University of California-San Diego and her MS and PhD degrees in optical sciences from the University of Arizona. She is the principal investigator of the automated desert vicarious calibration test site at Railroad Valley, NV, and is a participating member of the Committee on Earth Observation Satellites.

Kevin A. Burke is the project manager for MAIA at JPL. He received his BS degree in mechanical engineering from Cornell University and his MBA in entrepreneurship and finance from the UCLA Anderson School of Management. He specializes in mechanical systems engineering and was previously a product delivery manager on the Mars Curiosity Rover and flight systems manager for the Low-Density Supersonic Decelerators project.

Russell Chipman is a professor of optical sciences at the University of Arizona and a visiting professor at the Center for Optics Research and Education (CORE), Utsunomiya University, Japan. He received his BS degree in physics from MIT and his MS and PhD degrees in optical sciences from the University of Arizona. He specializes in polarization optical engineering, and collaborated with JPL on the design and development of the AirMSPI and AirMSPI-2 instruments.

Larry Di Girolamo is Blue Waters professor in the Department of Atmospheric Sciences at the University of Illinois at Urbana-Champaign. He received his BS degree in astrophysics from Queen's University at Kingston, and his MS and PhD degrees in atmospheric and oceanic sciences from McGill University. He leverages his experience on cloud mask development and aerosol and cloud validation on the MISR and MODIS science teams.

Michael J. Garay is a research scientist at JPL, with experience in radiative transfer, aerosol and cloud retrieval algorithm development, and validation for MISR. He received his BA degree in English literature and his BS degree in physics from the University of Toledo and his MS degree in atmospheric science from UCLA.

Sina Hasheminassab is an air quality specialist in the Science and Technology Advancement office at the South Coast Air Quality Management District, with expertise in air quality monitoring using *in situ* samplers and source apportionment modeling of ambient PM. He received his BS degree in chemical engineering from Sharif University of Technology (Tehran, Iran) and his MS and PhD degrees in environmental engineering from the University of Southern California.

Edward Hyer is a physical scientist at the Naval Research Laboratory in Monterey, CA. He received his BA degree in chemistry with sociology from Goucher College, and his MA and PhD degrees in geography from the University of Maryland. He is involved in a diverse array of research centered on observation and modeling of fires and smoke, and is a lead developer of the Fire Locating and Monitoring of Burning Emissions (FLAMBE) system.

Michael Jerrett is a professor and chair of the UCLA Fielding School of Public Health. He received his BSc degree in environmental science from Trent University, and his MA and PhD degrees in political environmental science and geography, respectively, from the University of Toronto. His expertise is in health impacts associated with exposure to air pollution and incorporation of satellite data products into PM exposure estimates.

Veljko Jovanovic is a senior member of the technical staff and technical group supervisor at JPL, with expertise in geometric calibration and digital photogrammetry. He received his BS degree in geodetic engineering from the University of Belgrade and his MS degree in geomatics engineering from Purdue University. He leads the MAIA science data system effort and is also deputy project manager for MISR.

Olga V. Kalashnikova is a research scientist at JPL, primarily working on applications of particle scattering theory and remote sensing observations to mapping aerosol properties using MISR and AirMSPI. She received her BS degree in physics from Kazakh State National University and her MS degree in physics and her PhD in astrophysical, planetary, and atmospheric science from the University of Colorado at Boulder.

Yang Liu is an associate professor in the Rollins School of Public Health at Emory University. He received his BS degree in environmental sciences and engineering from Tsinghua University, his MS degree in mechanical engineering from the University of California, and his PhD in environmental sciences and engineering from Harvard. He has developed PM2.5 exposure models using aerosol data from MISR, MODIS, and other satellite instruments and applied the results to health effects research.

Alexei I. Lyapustin is a research scientist at NASA Goddard Space Flight Center. He received his BS and MS degrees from Moscow State University, and his PhD from Space Research Institute, Moscow, Russia. He is expert in remote sensing of aerosol and land surface bidirectional reflectance from satellite sensors, radiative transfer theory with gaseous absorption and polarization, and is lead developer of the Multi-Angle Implementation of Atmospheric Correction (MAIAC) algorithm.

Randall V. Martin is a professor and Arthur B. McDonald chair of research excellence at Dalhousie University, and a research associate at the Smithsonian Astrophysical Observatory. He received his BS degree in engineering from Cornell, his MSc degree in environmental science from Oxford, and his MS and PhD degrees in engineering sciences from Harvard. He is the principal investigator of the Surface PARTiculate mAtter Network (SPARTAN), and leads the production of satellite-derived PM2.5 estimates for the Global Burden of Disease.

Abigail Nastan is a systems software engineer at JPL, specializing in applications development, science communications, and public outreach. She received her MS degree in planetary science from California Institute of Technology and her BS degree in international field geosciences from the University of Montana.

Bart D. Ostro is currently an environmental epidemiologist at the University of California, Davis. Prior to that, he was the chief of the Air Pollution Epidemiology Section for the California EPA. He received his State of California Certification in environmental epidemiology and his PhD in economics from Brown University. He has been involved in setting air quality standards and conducting epidemiologic studies around the world.

Beate Ritz is a professor of epidemiology at the UCLA Fielding School of Public Health with coappointments in Environmental Health Sciences and Neurology at UCLA. She received her MD degree and doctorate in medical sociology from the University of Hamburg, and her MPH and PhD in epidemiology from UCLA. Her primary research focuses on air pollution and adverse birth outcomes and child health.

Joel Schwartz is a professor of environmental epidemiology in the T.H. Chan School of Public Health at Harvard University. He received his PhD in theoretical physics from Brandeis University and his MD from the University of Basel. His research focuses on health impacts of air pollution, novel time-series and case-crossover methodologies, and development of geospatial air pollution models using satellite (MODIS and MISR) data.

Jun Wang is a professor in the College of Engineering at the University of Iowa. He received his BS degree in atmospheric dynamics from Nanjing Institute of Meteorology, his MS degree in mesoscale modeling from Institute of Atmospheric Physics, Chinese Academy of Sciences, and his PhD in atmospheric sciences from the University of Alabama–Huntsville. He has been studying PM air quality through a combination of satellite data (including MODIS and MISR), GEOS-Chem, and WRF-Chem.

Feng Xu is a research scientist at JPL, where he has been developing algorithms for coupled aerosol property and lower boundary retrievals and prototyping them for MAIA using MISR and AirMSPI data. He received his BS degree in thermal engineering and his MS degree in mechanical engineering from Shanghai University for Science and Technology, and his PhD in physics from the University of Rouen.